Anal. Methods Environ. Chem. J. 6 (4) (2023) 93-106

AMECJ

Research Article, Issue 4
Analytical Methods in Environmental Chemistry Journal
Journal home page: www.amecj.com/ir

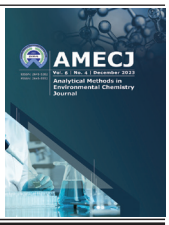

Removal of ethylene bisdithiocarbamate fungicides in wastewater and agricultural runoff by zinc oxide nanoparticles before analysis by HPLC and UV-Vis spectroscopy

Mahadi Danjuma Sani [a, c,*], V.D.N. Kumar Abbaraju [a], N.V.S. Venugopal [b], and Nura Umar Kura[c]

[a] *Department of Environmental Science, GITAM School of Science, GITAM (Deemed to be University), Visakhapatnam, A.P. India*

[b] *Department of Chemistry, GITAM School of Science, GITAM (Deemed to be University), Visakhapatnam, A.P. India*

[c] *Department of Environmental Science, Federal University Dutse, Jigawa State, Nigeria*

ARTICLE INFO:

Received 26 Jul 2023
Revised form 10 Oct 2023
Accepted 19 Nov 2023
Available online 30 Dec 2023

Keywords:
Removal,
Photocatalytic degradation,
Zinc oxide,
Ethylene bisdithiocarbamate,
High-performance liquid chromatography,
UV-Vis spectroscopy

ABSTRACT

This study developed an applied method based on the degradation to remove ethylene bisdithiocarbamate (EBDC) fungicides from wastewater and agricultural runoff by zinc oxide nanoparticles (ZnONPs). The synthesized ZnONPs were characterized using XRD for material crystallinity, scanning electron microscope (SEM) and particle size analysis (PSA) for surface structure, morphology and particle size (nm), respectively. The energy-dispersive X-ray spectroscopy (EDX) spectra confirmed the presence of zinc and showed that the synthesized zinc oxide nanoparticles were pure. Determination of the adsorption and photocatalytic degradation of Mancozeb (MCZ) fungicides based on ZnONPs was performed. Different amounts of ZnONPs were loaded into an MCZ fungicide solution in different concentrations. High-performance liquid chromatography (HPLC) and UV-Vis spectroscopy were used to determine the dithiocarbamate residue and the degradation efficiency of the synthesized particles. The particle size distribution of the synthesized ZnONPs was found to be in the range of 50-95 nm. At optimum conditions, with a ZnONPs dosage of 10 mg, (MCZ) fungicide concentration of 9.37 mg L^{-1}, and a duration of 60 minutes, the degradation efficiency was surpassed at more than 95%. Additionally, the nanoparticles demonstrated excellent reusability and maintained efficient activity for up to three cycles. It is crucial and significant to keep on exploring the intrinsic capabilities of abundant metal oxides like zinc oxide nanoparticles for environmental remediation and other applications.

1. Introduction

Ensuring equilibrium in our ecosystem is vital for the well-being of living and nonliving components. Using chemical pesticides plays a critical role in sustaining food production to meet the needs of a growing global population. However, it simultaneously poses risks to essential living organisms, including humans, and environmental frameworks. The residues of these pesticides were found in water [1], soil [2], food, and living systems [3, 4]. Pesticides are mainly used to destroy pests, living organisms with the same physiology and anatomy as other essential organisms like bees. These pesticides target body systems like the nervous

*Corresponding Author: Mahadi Danjuma Sani
Email: msani@gitam.in
https://doi.org/10.24200/amecj.v6.i04.251

system and other crucial systems in organisms, thereby disrupting and inhibiting the normal functioning of the physiology [5, 6]. The extensive and careless application of chemical pesticides on farms and agricultural products with little to zero knowledge of their proper application methods by most farmers brought about the unexpected. As a result, several synthetic chemical pesticides throughout history have found their way into water bodies through runoff, wind action, and many other processes. Studies have shown that most pesticides are persistent and can accumulate in a living system [7]. Dithiocarbamate pesticides like mancozeb (MCZ) are regarded as significant fungicides with applications worldwide by farmers from various countries [8]. Despite the wide application and acceptance of (MCZ) fungicides, it was found to be lethal and detrimental to off-target essential organism and human beings. Mancozeb was found to impart neurotoxicity, damaging mitochondria, and myofibril splitting [9], thyroid disruption [10], changes in glutathione and alterations in essential metal homeostasis [11], adverse effects on steroid production [12], ovarian injury and apoptosis [13], induce alteration in the development of hypothalamic systems that are essential for maturation of neuroendocrine system [14], disrupt mitochondria and bioenergetic activities in the body [15], affect male fertility [16] and induce behavioural deficit [17]. Although (MCZ) is widely accepted and used by farmers in many countries, these and many other reports have proven that the uncontrolled and excessive application of (MCZ) fungicide is a case for alarm. Therefore, there is an urgent and crucial need to devise a means through which the residues of these toxic pesticides can be reduced or degraded in the environment. Researchers employed several techniques to degrade pesticides in agricultural runoff or water in general, including conventional methods. However, the effectiveness, efficiency, and eco-friendliness of some of these techniques became another case of concern. Nanotechnology has brought a whole new view to the world of science, where tiny and unique products with a wide variety of essential properties are used in several sectors, including pharmaceuticals, medicine, agriculture, and environmental remediation. Gebre and Sendeku 2019 define nanotechnology as an interdisciplinary field of research involving nanoparticle synthesis, characterization, and application [18]. The evolving and modern technology consists of manipulating particles to form nanosized materials with various properties different from the parent material or raw materials with features like large surface area, light absorption, and suitable band gap energy that are essential today. The applications of nanoparticles in environmental remediation and cleanup cannot be overemphasized. Nanoparticles are effective photocatalytic agents [19, 20], possess great antimicrobial activity [21], act as biosensors [22], are active in the degradation of pesticides and other organic pollutants [23,24] and sound in the removal of heavy metals [25,26]if the amounts of heavy metals are more than the acceptable amounts (mentioned by WHO. Metal and metal oxide nanoparticles are important in wastewater remediation [27]. Furthermore, functionalized graphene oxide with bismuth and titanium oxide nanoparticles was revealed to effectively remove formaldehyde from the air by photocatalysis [28]. Moreover, xylene vapour was also neutralized in the air following photocatalysis in the presence of UV using bismuth oxide coupled graphene oxide nanomaterial [29]. Studies have shown that these nanoparticles have a special feature that helps in the adsorption, degradation, and removal of pesticides and other contaminants from wastewater [30,31]. Among the metal oxides or magnetic nanoparticles, zinc oxide ZnO was found to possess a large variety of essential properties that are significant in the field of wastewater remediation in addition to its abundance. Studies have reported the application of zinc oxide (NPs) in the degradation and photocatalytic degradation of pollutants and contaminants in the environment like quinclorac [32], polyethylene terephthalate [33], alizarin red dye [34], rhodamine B [35], hospital waste [31], amlodipine besylate [36], methylene blue and eosin yellow dye [37] and methylene blue and methyl orange [30]. Several studies have reported the photocatalytic activity

of ZnO (NPs), which was found to be an effective property in wastewater remediation. Moreover, ZnO (NPs) effectively and efficiently degrade toxic and volatile organic vapours (BTEX). Nagaraju et al. studied the efficiency of ZnO in the sensitivity of (BTEX). The investigation focused on the sensitivity and selectivity of toxic volatile organic vapours like benzene, toluene, ethylbenzene, and xylene (BTEX) under room-temperature conditions [38]. The findings revealed that (NPs) possess efficient activity in detecting BTEX, especially Xylene. Another study by [39] demonstrated an efficient visible light photocatalysis of BTEX in an aqueous solution. It was observed that ZnO nanorods were found to degrade more than 80% of the individual (BTEX) components. Therefore, ZnO (NPs) are also efficient in degrading and converting toxic compounds into harmless particles. Despite numerous studies focusing on the use of zinc oxide nanoparticles ZnO (NPs) for the degradation of contaminants in wastewater, there is a noticeable lack of attention given to their efficacy in degrading pesticides present in agricultural runoff. Only a few articles address pesticide degradation, with no known reports addressing dithiocarbamate (such as mancozeb) fungicides.

Consequently, this study aims to investigate the photocatalytic degradation of residues from the ethylene bis-dithiocarbamate mancozeb pesticide. This particular focus arises from the widespread use of mancozeb in agricultural practices and the presence of its residues in agricultural runoff. Furthermore, the research aims to address the potential environmental and health risks associated with mancozeb, given its known lethal and toxic effects on human health.

2. Materials and Methods

2.1. Instrumental, Materials and Reagents

All reagents and chemicals used for this research were of analytical grade with high purity. Zinc nitrate hexahydrate ($Zn(NO_3)_2.6H_2O$, 98%, CAS No.: 10196-18-6), and sodium hydroxide (NaOH, 98%, CAS No.: 1310-73-2) were purchased from Merck Specialties Private Limited, Mumbai, India. Ethylene bisdithiocarbamate fungicide (Mancozeb fungicide, 75% WP) was purchased from a farmers' market in Vishakapatnam, Andhra Pradesh, India. Millipore Pure water (DI water) was used throughout the work. The Powder X-ray diffraction (PXRD) analysis utilized a Brucker D8 advance facility with a coupled two theta/theta scanning type and mode, employing continuous scanning. Scanning Electron Microscopy-Energy Dispersive X-ray Spectroscopy (SEM-EDAX) was performed using a Jeol 6390 LA/OXFORD XMXN instrument with an accelerating voltage ranging from 0.5 to 30 kV, a magnification of 300,000 times, and a tungsten filament. UV-Vis analysis was conducted using a Shimadzu 1800 instrument, while High-Performance Liquid Chromatography (HPLC) analysis employed an Agilent Technologies 1260 Infinity machine equipped with a UV detector, column oven, electric sample valve, and a Phenomenex Zodiac C18 reversed-phase column (5.0 µm, 150 × 4.60 mm, i.d.).

2.2. Synthesis of ZnO Nanoparticle

Zinc oxide nanoparticle ZnO nanoparticle was prepared or synthesized following a simple and friendly co-precipitation/wet chemical method as modified from the work of [40]we synthesized Hexagonal Zinc oxide (ZnO. Figure 1 shows the stepwise procedure of the synthesis.

Zinc nitrate hexahydrate was employed as a precursor, along with sodium hydroxide and starch serving as precipitating/capping and stabilizing agents. A 0.1 M concentration of zinc nitrate hexahydrate was prepared by dissolving 9.468 g of ($Zn(NO_3)_2.6H_2O$) in 500 ml of double DI water/Millipore water. Additionally, 1% starch solution was prepared and dissolved in the zinc nitrate solution, with continuous stirring until a cloudy solution was formed. Subsequently, drops of 0.2 M concentration of sodium hydroxide were added to the solution under constant stirring, leading to the formation of precipitates. The stirring process continued for 3 hours until a white precipitate of zinc hydroxide ($Zn(OH)_2$) was formed. The solution was left to settle for an hour and then centrifuged at 5000 rpm for 10 minutes. The supernatant liquid was discarded, and the obtained particles were oven-dried at 100°C for

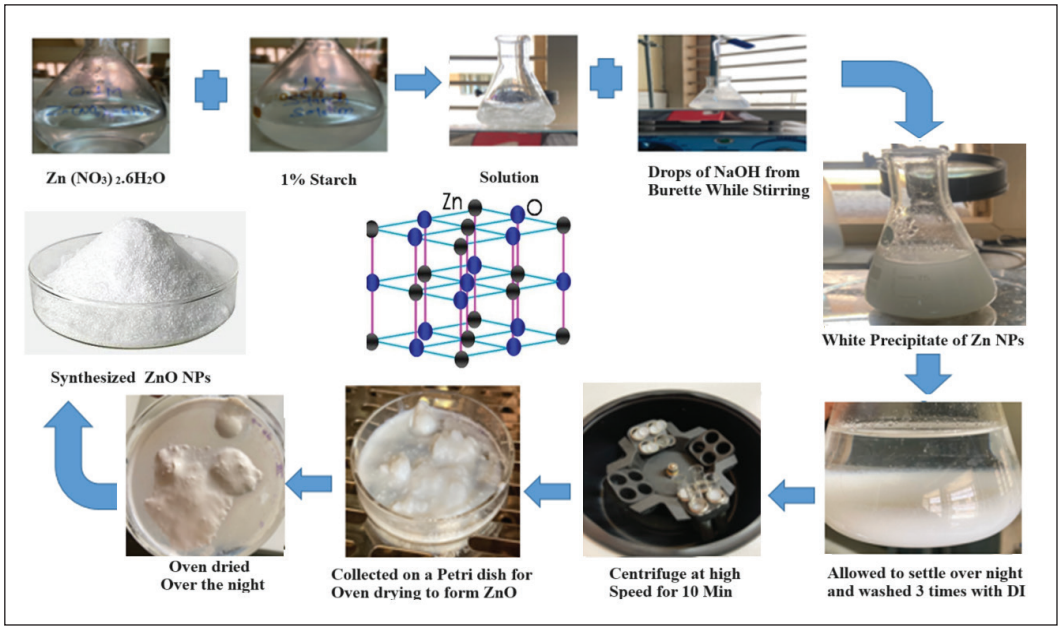

Fig. 1. Synthesis of Zinc oxide Nanoparticles

a few hours to produce the Zn (OH) powder. Later, the powder underwent calcination at 400°C for 3 hours in a muffle furnace to yield ZnO (NPs).

2.3. Characterizations

The synthesized zinc oxide nanoparticles were characterized using X-ray Diffraction (XRD) to determine the crystal structure, crystallite size, and pure phase formation. Scanning Electron Microscopy (SEM) was employed to ascertain the structure and surface morphology of the as-synthesized NPs. Energy Dispersive X-ray Spectroscopy (EDX) was utilized for elemental composition analysis, and particle size analysis was conducted to determine the size of the synthesized nanoparticles.

2.4. Preparation of standard concentrations of Mancozeb Fungicide

The preparation of standard concentrations of the ethylene bis-dithiocarbamate fungicide mancozeb was meticulously carried out in the Environmental Biotechnology Laboratory of GITAM University. Four different concentrations were carefully prepared using Millipore deionized water.

2.5. Adsorption and Photocatalytic Degradation of Mancozeb

This was conducted from 11 pm to 4 pm under natural solar radiation at room temperature to determine the adsorption and photocatalytic activity of ZnO (NPs) on (MCZ) fungicide. Different amounts of (NPs) were loaded into a known concentration of (MCZ) fungicide solution and tagged as; SA, SB,

Table 1. Sample setup containing pesticides and the amounts of loaded nanoparticles

Sample Code	Amount of (NPs)	Initial Concentration before degradation
SA	10 mg	2.0 mg L^{-1}
SB2	5 mg	4.0 mg L^{-1}
SB2	10 mg	4.0 mg L^{-1}
SC1	5 mg	9.4 mg L^{-1}
SC2	10 mg	9.4 mg L^{-1}
SD1	5 mg	15.0 mg L^{-1}
SD2	10 mg	15.0 mg L^{-1}

SC, and SD, respectively (Table 1).

For each batch, the solutions were stirred in the dark for 30 minutes to attain adsorption-desorption equilibrium before exposure to natural solar irradiation at room temperature. After exposure to natural solar irradiation, 10 mL of the solution was sampled every 20 minutes until 120 minutes and then centrifuged at 4000 rpm for 10 minutes to gather the photocatalyst. Each resulting supernatant liquid was collected, labelled, and subjected to UV-visible spectroscopy for absorbance and concentration determination using the Shimadzu 1800 UV spectrophotometer. UV-visible spectroscopy relies on the principles outlined in Beer's Law for quantifying the concentration of a substance in a solution. Beer's Law asserts that the concentration of a substance within a solution is directly proportional to the amount of light absorbed or transmitted through the solution. This technique is frequently employed for gauging the concentration of a substance in a solution, this principle involves measuring the substance's absorbance at a designated wavelength. Also, the UV absorbance of the samples were determined at a wavelength of 190-400 nm. The maximum absorbance ƛmax was obtained at a wavelength of 240 nm. The concentration at time t of each round of the experiment was determined following standard procedure using standard MZC solutions prepared by serial dilution method at ƛmax. The same procedure was applied for the control without (NPs).

The effects of time, amount of (NPs), and initial concentration of pesticide were optimized to achieve better results. The final results were exposed to (HPLC) analysis to ascertain the final concentration of the pesticide in the supernatant liquid. HPLC is an important analytical technique/tool for the separation, identification, and quantification of particles in liquid samples. It involves applying high pressure to the mobile phase, allowing for faster and more efficient separations. The same procedure was repeated multiple times after washing the collected/ used nanoparticles to study the recoverability and reusability of the (NPs). The degradation efficiency of the zinc oxide nanoparticles was computed using the following formula;

$$\text{Degradation efficiency} = \frac{Co - Ct}{Co} \times 100$$

Where Co = initial concentration of MCZ in mg L^{-1}
Ct = Concentration at time t (observed concentration in the supernatant) in mg L^{-1}

3. Results and Discussion

3.1. Formation of Zinc oxide Nanoparticle.

Zinc oxide nanoparticle was successfully synthesized through the co-precipitation method using zinc nitrate hexahydrate as a precursor, sodium hydroxide, and starch as precipitating/capping and stabilizing agents. This process follows the possible mechanism of formation of ZnO (NPs) as reported

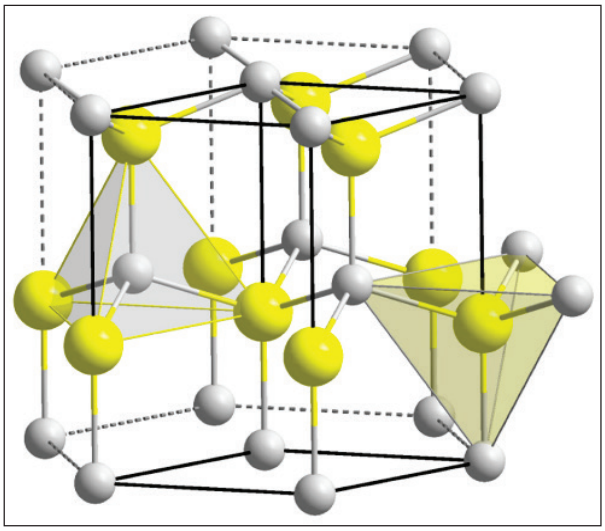

Fig. 2. Zinc oxide Nanoparticle

by [RS 1] which begins with nucleation and growth by diffusion, followed by interparticle growth and ripening. Figure 2 shows the white pow2der zinc oxide nanoparticles synthesized which was later confirmed through characterization by XRD, SEM, and particle analysis.

3.2. Characterization of the Zinc Oxide Nanoparticles

3.2.1.Scanning Electron Microscopy Analysis SEM

The surface morphology and structure of the synthesized zinc oxide nanoparticles were determined using (SEM) analysis. Figure 3 shows the images obtained from (SEM) analysis of the as-synthesized (NPs). It can be observed that the structure and surface morphology of the synthesized (NPs) are presented in different sizes ranging from 1µm to 100 nm. The last image on the bottom right confirms the particle size to be below 100 nm. The sizes of the particles are almost similar as can be observed in Fig. 4 above. The spherical and hexagonal structure of the synthesized particle is in agreement with the findings of [RS2].

3.2.2.Energy Dispersive X-ray Spectroscopy EDX

Energy Dispersive X-ray spectroscopy (EDX) provides the elemental composition of the synthesized nanoparticles with peaks located between 0.5 and 9.0. It can be observed in Figure 4 that the peaks for zinc and oxygen are vividly clear as shown on the spectrum, which can be regarded as the presence of the elements that make up zinc oxide nanoparticles.

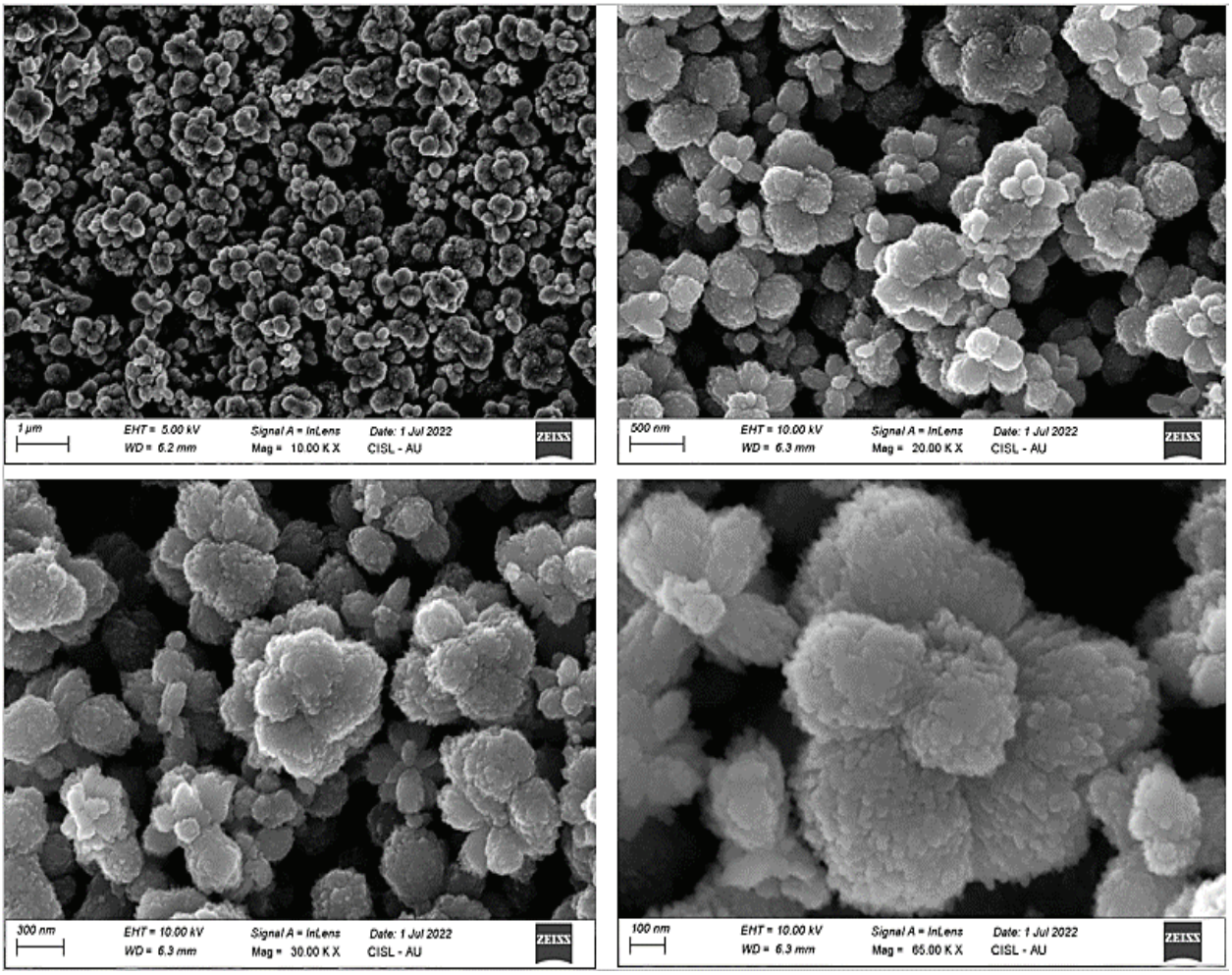

Fig.3. Scanning Electron Microscope Images showing the surface morphology and shape of the synthesized nanoparticles

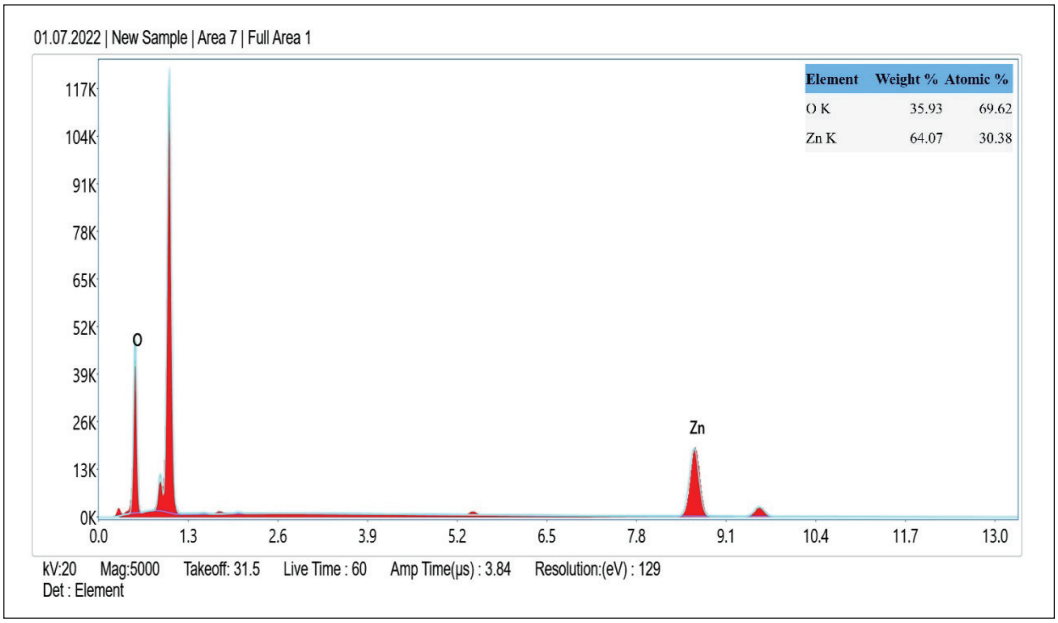

Fig. 4. EDX showing the elemental composition of the synthesized nanoparticles

Although other peaks are available in the spectrum which indicates the presence of other particles, zinc and oxygen were found to possess the strongest peaks.

3.2.3.PXRD Analysis

The crystalline structure of the synthesized zinc oxide nanoparticles is provided in Figure 5 below with peaks corresponding to different crystal planes. With special reference to JCPDS card number 89-0510, the diffraction peaks obtained for the synthesized zinc oxide nanoparticles confirm the formation of the hexagonal wurtzite phase of ZnO nanoparticles. The peaks at 31.640°, 34.291°, and 36.083° correspond to (100), (002), and (101) planes of hexagonal crystal patterns of ZnO respectively. The peaks are also in agreement with multiple reported literature [30], [31]. The crystallite size of the particles were at a range of 50-95nm.

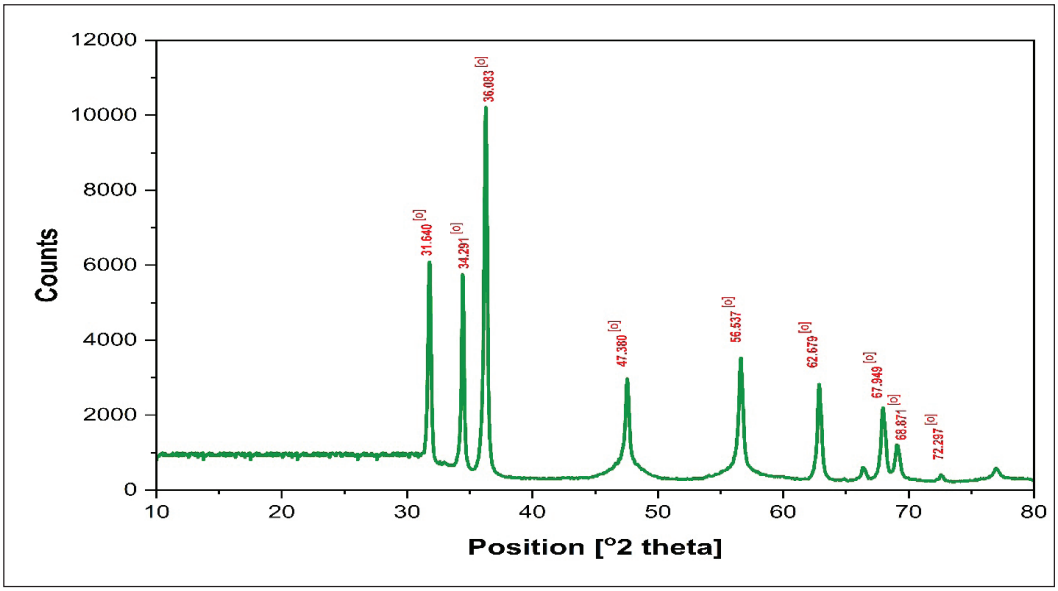

Fig. 5. XRD spectra showing the peaks for the synthesized ZnO NPs

3.3. Photocatalytic activity

Photocatalytic degradation or activity of zinc oxide nanoparticles using ethylene bis-dithiocarbamate fungicides was evaluated. UV-visible spectroscopy and HPLC analysis were used to determine the initial concentration and concentration at time (t). The degradation efficiency of the synthesized particles was determined.

3.3.1. UV-Visible Spectroscopy

Shimadzu UV-1800 spectrophotometer was used in the Environmental Biotechnology Laboratory of the Environmental Science Department, GITAM University. Figure 6 above shows the UV spectrum with absorbance at different time intervals for the sample; SC-2. It can be observed that there is a sharp decrease in the absorbance around the λmax between the initial SC-2 concentration and concentration at time t, which is considered a sharp decrease in the concentration of pesticides in the solution. It can be observed that the lowest absorbance was recorded at 60 minutes/1 hour. After optimization for time, initial concentration of pesticide, and the amount of the nanoparticle or photocatalyst, this sample set-up was found to possess the highest activity against the pesticide. The findings revealed in this work agree with multiple findings in literature where pure and doped ZnO (NPs) were reported to significantly decrease the absorbance of multiple pesticides including; quinclorac herbicide [32], imidacloprid pesticide [RS3]we developed a Z-scheme photocatalyst system consisting of PANI/ZnO-CoMoO4 for degradation photocatalytic processes. The structural composition and morphologies of the PANI/ZnO-CoMoO4 nanocomposite were analyzed by FTIR, FESEM-EDS, and XRD techniques. Subsequently, the pesticide-degradation experiments were performed for the degradation of imidacloprid (IM, and lambda-cyhalothrin pesticide [RS4].

3.3.2. HPLC Analysis

High-Performance Liquid Chromatography, also known as High-Pressure Liquid Chromatography, was used for the final quantification of the pesticide concentration. The experiment was conducted at Biofact Research PVT. Limited at Visakhapatnam, Andhra Pradesh. The instrument name is HPLC Agilent 1260 infinity with an instrument code of BFR/EQ/0487. Agilent HPLC (1260 Infinity II) equipped with UV detector, column oven, electric sample valve, Phenomenex Zodiac C18 reversed-phase column (5.0 µm, 150 × 4.60 mm, i.d).

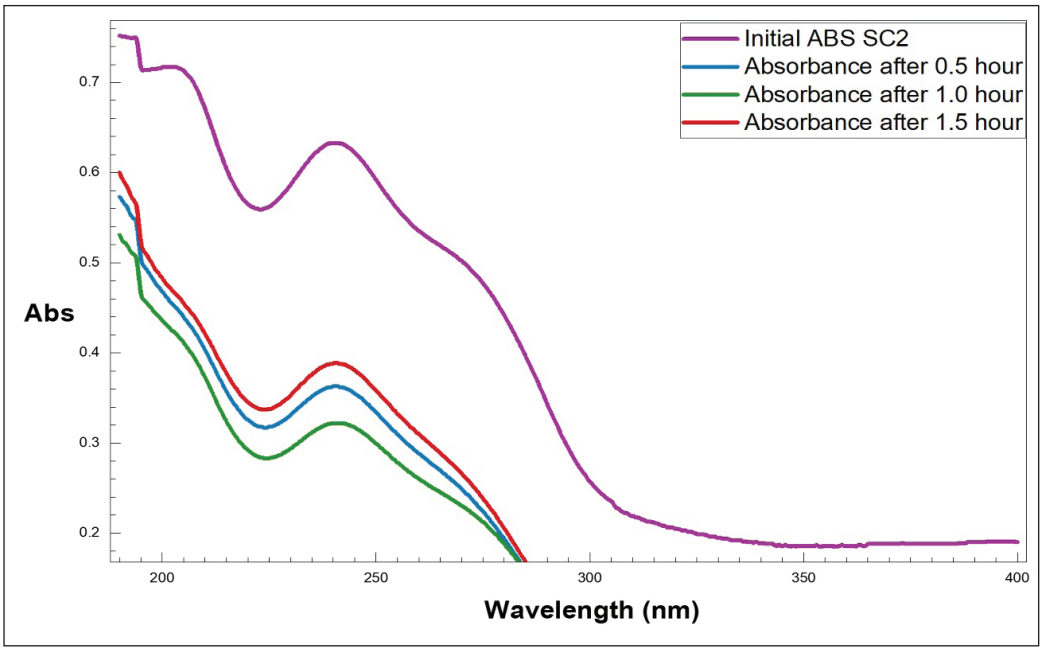

Fig. 6. UV absorbance in the batch photocatalytic experiment of SC2

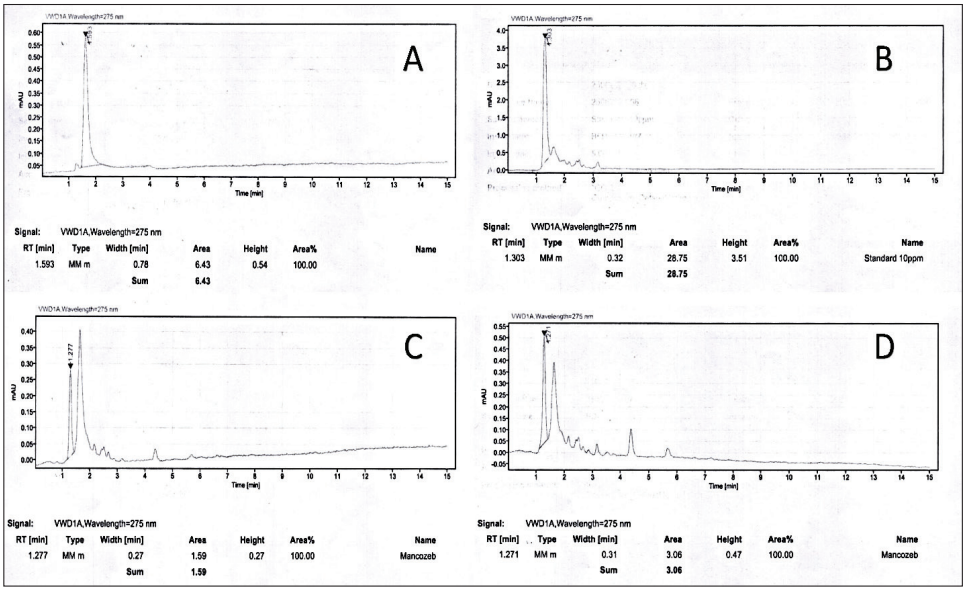

Fig. 7. HPLC curves showing; A) blank, B) 10 mg L^{-1} standard, C) SC-2, and D) SD-2

The data were processed by Agilent 2D- LC-solution software. Determination of mancozeb concentration was performed using a mobile phase at a flow rate of 1.0 mL min^{-1}. Ten microliters of the sample were injected, and it was detected at 275 nm under 25 °C. Figure 7 below revealed the HPLC curves of the analysis with the retention time, area, width, and height for each curve. As can be observed from caption B of the figure, the area of 10 mg L^{-1} standards was revealed to be 28.75 whereas, captions C and D show that of SC-2 and SD-2 to be 1.59 and 3.06 respectively. The final concentration at optimum conditions was determined from the HPLC curves.

Also, Table 2 and Figure 8, it can be observed that the effect of the nanoparticles on the degradation of (MCZ) pesticides differs at various concentrations of the pesticides and the amount of zinc oxide nanoparticles used. This is a result of numerous factors which include the initial concentration of the pesticide, the dosage of the photocatalyst, irradiation time and other factors. However, the findings revealed that increasing the dosage of the photocatalyst has shown a greater degradation efficiency. Due to Figure 8, it can be observed that SB-2, SC-2, and SD-2 with a 10 mg dosage of the photocatalyst have shown greater efficiency than their counterparts with the same initial pesticide concentration. Research indicates that elevating the catalyst quantity leads to increased pesticide degradation in the solution, reaching a point where degradation plateaus and/or diminishes, likely attributed to reduced light penetration [RS5] residential, and commercial applications. The release of chlorpyrifos into water and wastewater sources may affect human health because of its chronic toxicity to aquatic organisms. Therefore, its degradation seems necessary. The present study aimed to investigate the photocatalytic efficiency of biochar nanocomposite based on grapefruit skin modified with Fe3O4 and CdS nanoparticles (biochar/CdS-Fe3O4. The initial concentration of the pesticide was also found to affect the degradation efficiency. SC-2 with 9.37 mg L^{-1} pesticides has shown better efficiency than SA and SB samples with lower concentrations and SD samples with higher concentrations. Light penetration is crucial for photocatalysis and increasing pesticide concentration may diminish light penetration and hence the photocatalytic activity. Therefore,

the gradual increase in efficiency from SA to SC may be a result of other factors whereas, the decreasing efficiency observed in SD samples may be attributed to lower light penetration. The best degradation efficiency was achieved when 10 mg of NPs dose was applied to 9.37 mg L^{-1} of the (MCZ) solution for an hour.

The degradation efficiency of the pesticide using the synthesized photocataly were presented in Figure 9 and Table 3. The percentage degradation/ degradation efficiency as computed is presented in the figure. It can be observed that at optimum conditions, SC-2 was found to possess the highest efficiency followed by SD-2 and SB-2. Moreover, SB-1 with 4 mg L^{-1} initial pesticide concentration and 5.0 mg dosage of the photocatalyst was revealed to possess lower degradation efficiency. The reusability and recoverability of the sample (NPs) were studied after 7 rounds of experiments under optimum conditions. It was revealed that, at optimum conditions, the (NPs) were shown to be active and efficient up to 3 rounds of the degradation experiment which later on began to slightly decline.

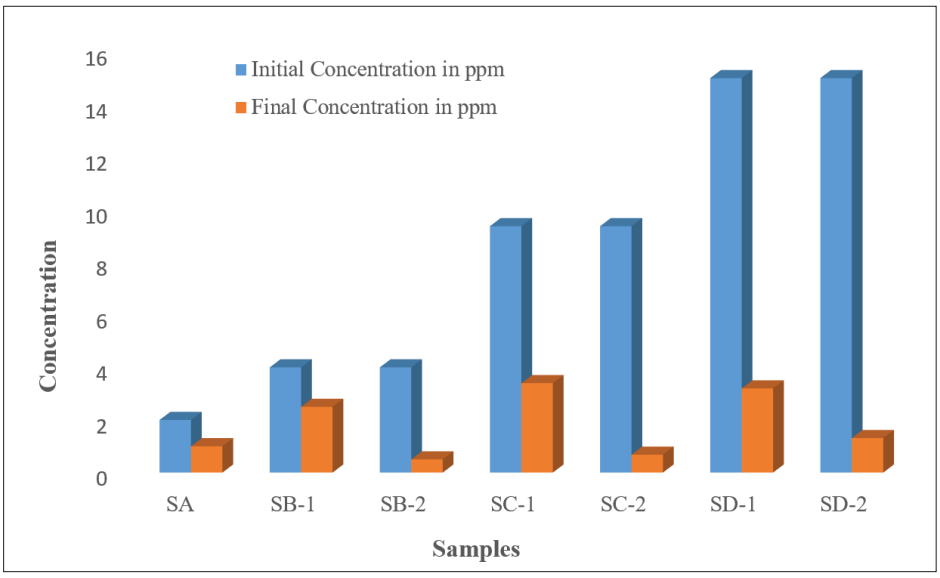

Fig. 8. The initial and final concentrations of MCZ pesticide degradation

Table 2. Initial and final concentrations of mancozeb fungicide as detected by HPLC analysis at an optimal time condition

Sample Code	Amount of NPs	Initial Concentration before degradation	Final Concentration after degradation	Degradation efficiency
SA	10 mg	2.0 mg L^{-1}	1.0 mg L^{-1}	50%
SB2	5 mg	4.0 mg L^{-1}	2.5 mg L^{-1}	44.4%
SB2	10 mg	4.0 mg L^{-1}	0.5 mg L^{-1}	88.8%
SC1	5 mg	9.4 mg L^{-1}	3.4 mg L^{-1}	63.71%
SC2	10 mg	9.4 mg L^{-1}	0.68 mg L^{-1}	92.70%
SD1	5 mg	15.0 mg L^{-1}	3.2 mg L^{-1}	78.66%
SD2	10 mg	15.0 mg L^{-1}	1.31 mg L^{-1}	91.2%

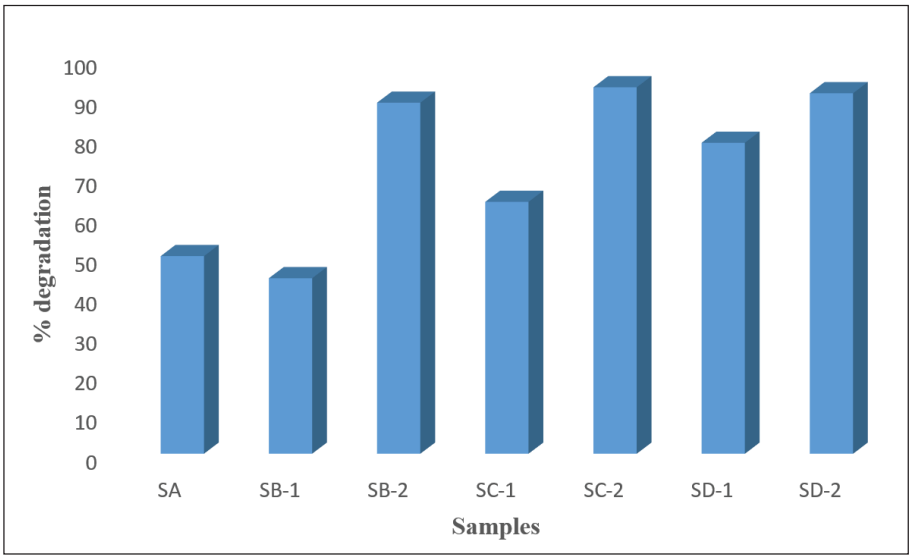

Fig. 9. Degradation efficiency at various experimental conditions for the removal of MCZ

Table 3. Comparison between the current method and the reported electrochemical method in the literature

S/N	Method	degradation %	Source
1	Photocatalytic degradation using NPs	.92%	Current work
2	The electrochemical method under UV	67%	[RS6]

4. Conclusions

In this study, a suitable method was established for the photocatalytic degradation of (MCZ) in wastewater and agricultural runoff using Zinc Oxide Nanoparticles. The (XRD) pattern and (SEM) studies have shown that zinc oxide nanoparticles are Rhombohedral in structure. The (EDAX) spectra confirmed the presence of zinc element and showed that the synthesized zinc oxide nanoparticles were pure. Different amounts of (NPs) were loaded into a preconcentrated (MCZ) fungicide solution of different concentrations. HPLC and UV analysis were used to determine the degradation efficiency of the synthesized particles. The particle size distribution of the synthesized zinc oxide NPs was found to be in the range of 50-95 nm. At optimum conditions of 10 mg NPs dosage, 9.37 mg L^{-1} concentration of (MCZ) fungicide, and 60 minutes, the degradation efficiency was revealed to be above 92%. Moreover, the (NPs) were shown to possess great recoverability and reusability with efficient activity up to 3 rounds. It is crucial and significant to keep on exploring the intrinsic capabilities of abundant metal oxides like zinc oxide nanoparticles for environmental remediation and other applications.

5. Acknowledgement

The authors sincerely thank the School of Science, GITAM (deemed to be a University) for giving support and facilities for completing the research work

6. References

[1] R. Garg, R. Gupta, N. Singh, A. Bansal, Eliminating pesticide quinalphos from surface waters using synthesized GO-ZnO nanoflowers: Characterization, degradation pathways and kinetic study, Chemosphere, 286 (2022) 131837. https://doi.org/10.1016/J.CHEMOSPHERE.2021.131837.

[2] C. M. Martínez-Escudero, I. Garrido, P. Flores, P. Hellín, F. Contreras-López, J. Fenoll, Remediation of triazole, anilinopyrimidine,

strobilurin and neonicotinoid pesticides in polluted soil using ozonation and solarization, J. Environ. Manage., 310 (2022) 114781.https://doi.org/10.1016/J.JENVMAN.2022.114781.

[3] F. Hüesker, R. Lepenies, Why does pesticide pollution in water persist?, Environ. Sci. Policy, 128 (2022)185–193. https://doi.org/10.1016/J.ENVSCI.2021.11.016.

[4] A. Alsendi, A. A. Kareem, M. Havasi, G. Golmohammadi, A study on the toxicity and sublethal concentrations of three insecticides on the population dynamics of green lacewing chrysoperla carnea stephens, Arab J. Plant Prot., 41 (2023) 28-36. https://doi.org/10.22268/AJPP-41.1.028036.

[5] E. Gök, E. Deveci, Histopathological, immunohistochemical and biochemical alterations in liver tissue after fungicide-mancozeb exposures in Wistar albino rats, Acta Cirúrgica Bras., 37 (2022) e370404. https://doi.org/10.1590/ACB370404.

[6] S. Kumar, T. R. Baggi, T. Al-Zughaibi, Forensic toxicological and analytical aspects of carbamate poisoning-A review, J. Forensic Leg. Med., 92 (2022)102450. https://doi.org/10.1016/J.JFLM.2022.102450.

[7] Y. Bai, X. Ruan, J. P. van der Hoek, Residues of organochlorine pesticides (OCPs) in aquatic environment and risk assessment along Shaying River, China, Environ. Geochem. Health, 40 (2018) 2525–2538. https://doi.org/10.1007/S10653-018-0117-9/TABLES/5.

[8] J. S. Aprioku, B. Pharm, A. M. Amamina, A. Nnabuenyi, Mancozeb-induced hepatotoxicity: protective role of curcumin in rat animal model, Toxicol. Res. (Camb), 12 (2023) 107–116. https://doi.org/10.1093/TOXRES/TFAC085.

[9] O. J. Stephenson, L. D. Trombetta, Comparative effects of Mancozeb and Disulfiram-induced striated muscle myopathies in Long-Evans rats, Environ. Toxicol. Pharmacol., 74, (2020) 103300. https://doi.org/10.1016/J.ETAP.2019.103300.

[10] F. Bano, B. Mohanty, Thyroid disrupting pesticides mancozeb and fipronil in mixture caused oxidative damage and genotoxicity in lymphoid organs of mice, Environ. Toxicol. Pharmacol., 79 (2020)103408. https://doi.org/10.1016/J.ETAP.2020.103408.

[11] B. R. Kistinger, D. Hardej, The ethylene bisdithiocarbamate fungicides mancozeb and nabam alter essential metal levels in liver and kidney and glutathione enzyme activity in liver of Sprague-Dawley rats, Environ. Toxicol. Pharmacol., 92 (2022) 103849. https://doi.org/10.1016/J.ETAP.2022.103849.

[12] N. Atmaca, Effects of mancozeb, metalaxyl and tebuconazole on steroid production by bovine luteal cells in vitro, Environ. Toxicol. Pharmacol., 59 (2018) 114–118. https://doi.org/10.1016/J.ETAP.2018.03.009.

[13] J. Bao, Y. Zhang, R. Wen, L. Zhang, X. Wang, Low level of mancozeb exposure affects ovary in mice, Ecotoxicol. Environ. Saf., 239 (2022)113670. https://doi.org/10.1016/J.ECOENV.2022.113670.

[14] Y. Morales-Ovalles, Developmental exposure to mancozeb induced neurochemical and morphological alterations in adult male mouse hypothalamus, Environ. Toxicol. Pharmacol., 64 (2018)139–146. https://doi.org/10.1016/J.ETAP.2018.10.004.

[15] M. A. Saraiva, Mancozeb impairs mitochondrial and bioenergetic activity in Drosophila melanogaster, Heliyon, 7 (2021) e06007. https://doi.org/10.1016/J.HELIYON.2021.E06007.

[16] E. E. Elsharkawy, M. A. El-Nasser, A. A. Bakheet, Mancozeb impaired male fertility in rabbits with trials of glutathione detoxification, Regul. Toxicol. Pharmacol., 105 (2019) 86–98. https://doi.org/10.1016/J.YRTPH.2019.04.012.

[17] A. Harrison Brody, E. Chou, J. M. Gray, N. J. Pokyrwka, K. M. Raley-Susman, Mancozeb-induced behavioral deficits precede structural neural degeneration, Neurotoxicol., 34 (2013) 74–81. https://doi.org/10.1016/J.

NEURO.2012.10.007.

[18] S. H. Gebre, M. G. Sendeku, New frontiers in the biosynthesis of metal oxide nanoparticles and their environmental applications: an overview, SN Appl. Sci., 1 (2019) 1–28. https://doi.org/10.1007/S42452-019-0931-4

[19] E. Hannachi, Synthesis, characterization, and evaluation of the photocatalytic properties of zinc oxide co-doped with lanthanides elements, J. Phys. Chem. Solids, 170 (2022) 110910. https://doi.org/10.1016/J.JPCS.2022.110910.

[20] P. Akhter, Efficient visible light assisted photocatalysis using ZnO/TiO2 nanocomposites, Mol. Catal., 535 (2023) 112896. https://doi.org/10.1016/J.MCAT.2022.112896.

[21] R. M. Abdelhameed, O. M. Darwesh, M. El-Shahat, Titanium-based metal-organic framework capsulated with magnetic nanoparticles: Antimicrobial and photocatalytic degradation of pesticides, Micropor. Mesopor. Mater., 354 (2023)112543.b https://doi.org/10.1016/J.MICROMESO.2023.112543.

[22] L. Zhang, Silicon quantum dots and MOFs hybrid multicolor fluorescent nanosensor for ultrasensitive and visual intelligent sensing of tetracycline, Coll. Surf. A Physicochem. Eng. Asp., 652 (2022) 129853. https://doi.org/10.1016/J.COLSURFA.2022.129853.

[23] M. Samadifar, Y. Yamini, M. M. Khataei, Magnetically solid-phase extraction of diazinon and chlorpyrifos pesticides in vegetables using covalent triazine-based framework incorporated chitosan nanocomposite, J. Food Compos. Anal., 118 (2023) 105158. https://doi.org/10.1016/J.JFCA.2023.105158.

[24] S. Amiri, M. Anbia, Enhanced degradation of diazinon in aqueous solution using C-TiO2/g-C3N4 nanocomposite under visible light: Synthesis, characterization, kinetics, and mechanism studies, Mater. Res. Bull., 16 5(2023)112289. https://doi.org/10.1016/J.materresbull.2023.112289.

[25] M. Arjomandi, H. Shirkhanloo, A Review: Analytical methods for heavy metals determination in environment and human samples, Anal. Methods Environ. Chem. J., 2 (2019) 97–126. https://doi.org/10.24200/amecj.v2.i03.73.

[26] S. Golkhah, H. Zavvar Mousavi, Removal of Pb (II) and Cu (II) Ions from aqueous solutions by cadmium sulfide Nanoparticles, Int. J. Nanosci. Nanotechnol. 13 (2017) 105-117. https://www.ijnnonline.net/article_25609.html

[27] A. Ali, S. Ahmed, Green Synthesis of Metal, Metal Oxide Nanoparticles, and Their Various Applications, Springer Book, pages 1-45, 2018. https://doi.org/10.1007/978-3-319-48281-1_115-1.

[28] M. M. Asl, N. Mansouri, S. A. R. H. S. Mirzahosseini, F. Atabi, Functionalized graphene oxide with bismuth and titanium oxide nanoparticles for efficiently removing formaldehyde from the air by photocatalytic degradation–adsorption process, J. Anal. Test., (2023) 1–15. https://doi.org/10.1007/s41664-023-00272-0

[29] A. Faghihi-Zarandi, J. Rakhtshah, B. Bahrami Yarahmadi, A rapid removal of xylene vapor from environmental air based on bismuth oxide coupled to heterogeneous graphene/ graphene oxide by UV photo-catalectic degradation-adsorption procedure, J. Environ. Chem. Eng., 8 (2020)104193. https://doi.org/10.1016/j.jece.2020.104193

[30] R. R. Wary, S. Baglari, D. Brahma, U. K. Gautam, P. Kalita, M. B. Baruah, Synthesis, characterization, and photocatalytic activity of ZnO nanoparticles using water extract of waste coconut husk, Environ. Sci. Pollut. Res., 29 (2022) 42837–42848. https://doi.org/10.1007/s11356-022-18832-9

[31] A. M. Tatagar, J. I. Moodi, J. C. Abbar, M. A. Phaniband, Photocatalytic activity and anti-microbial application of synthesized Zinc oxide nanoparticles (ZnO Nps) towards

remediation of hospital waste water (HWW), Mater. Today Proc., 49 (2022) 699–702. https://doi.org/10.1016/j.matpr.2021.05.176

[32] V. N. Rao, N. V. S. Venu Gopal, T. B. Patrudu, Zinc oxide nanoparticles catalytic activity for the degradation of quinclorac herbicide residues in water, Bull. Monum., 21(2020)161. http://bulletinmonumental.com/

[33] Y. Li, K. Li, M. Li, M. Ge, Zinc-doped ferrite nanoparticles as magnetic recyclable catalysts for scale-up glycolysis of poly(ethylene terephthalate) wastes, Adv. Powder Technol., 33 (2022)103444. https://doi.org/10.1016/J.APT.2022.103444.

[34] B. Sowjanya, U. Sirisha, A. Suhasini Juttuka, S. Matla, P. King, M. Vangalapati, Synthesis and characterization of zinc oxide nanoparticles: It's application for the removal of alizarin red S dye, Mater. Today Proc., 62 (2022) 3968-3972. https://doi.org/10.1016/j.matpr.2022.04.576

[35] S. Rajendrachari, P. Taslimi, A. C. Karaoglanli, O. Uzun, E. Alp, G. K. Jayaprakash, Photocatalytic degradation of Rhodamine B (RhB) dye in waste water and enzymatic inhibition study using cauliflower shaped ZnO nanoparticles synthesized by a novel One-pot green synthesis method, Arab. J. Chem., 14 (2021)103180. https://doi.org/10.1016/J.ARABJC.2021.103180.

[36] E. Alizadeh, H. Baseri, Catalytic degradation of Amlodipine Besylate using ZnO, Cu doped ZnO, and Fe doped ZnO nanoparticles from an aqueous solution: Investigating the effect of different parameters on degradation efficiency, Solid State Sci., 78 (2018) 86–94. https://doi.org/10.1016/j.solidstatesciences.2018.02.010

[37] K. Rambabu, G. Bharath, F. Banat, P. L. Show, Green synthesis of zinc oxide nanoparticles using Phoenix dactylifera waste as bioreductant for effective dye degradation and antibacterial performance in wastewater treatment, J. Hazard. Mater., 402 (2021) 123560. https://doi.org/10.1016/j.jhazmat.2020.123560.

[38] P. Nagaraju, Y. Vijayakumar, M. V. Ramana Reddy, Room-temperature BTEX sensing characterization of nanostructured ZnO thin films, J. Asian Ceram. Soc., 7 (2019) 141–146. https://doi.org/10.1080/21870764.2019.1579401.

[39] J. Al-Sabahi, T. Bora, M. Al-Abri, J. Dutta, Efficient visible light photocatalysis of benzene, toluene, ethylbenzene and xylene (BTEX) in aqueous solutions using supported zinc oxide nanorods, PLOS One, 12 (2017) e0189276. https://doi.org/10.1371/journal.pone.0189276

[40] S. M. Nampoothiri, V. Chandran, E. M. Mohammed, R. Francis, Preparation and Characterization of Zinc Oxide(ZnO) Nanoparticles via Co-precipitation Method, Int. J. Sci. Res. Pap. Multidiscip. Stud., 5 (2019) 56–61. https://www.isroset.org/pdf_paper_view.php?paper_id=1447&8-IJSRMS-02507.pdf

Note: RS1-RS6 showed in Supplementary Material (ESM)